Estuarine, Coastal and Shelf Science 261 (2021) 107557

Contents lists available at ScienceDirect

Estuarine, Coastal and Shelf Science

journal homepage: www.elsevier.com/locate/ecss

Elemental composition of illicia and otoliths and their potential application to age validation in white anglerfish (*Lophius piscatorius* linnaeus, 1758)

Deirdre Brophy [a,*], Sílvia Pérez-Mayol [b], Roxanne Duncan [a,c], Karin Hüssy [d], Audrey J. Geffen [e], Hans D. Gerritsen [c], Maria Ching Villanueva [f], Beatriz Morales-Nin [b]

[a] Marine and Freshwater Research Centre, Galway Mayo Institute of Technology, Dublin road, Galway, H91 T8NW, Ireland
[b] IMEDEA (CSIC-UIB), C/ Miquel Marquès, 21, 07190, Esporles, Illes Balears, Spain
[c] Marine Institute, Rinville, Oranmore, Galway, H91 R673, Ireland
[d] National Institute of Aquatic Resources, Technical University of Denmark, Kemitorvet, 2800, Kgs. Lyngby, Denmark
[e] Department of Biological Sciences, University of Bergen, PO Box 7800, 5020, Bergen, Norway
[f] IFREMER, Unité écologie et modèles pour l'halieutique Ifremer, EMH, F-29280, Plouzané, France

ARTICLE INFO

Keywords:
Age validation
Illicium
Otolith microchemistry
Seasonality
Anglerfish
Lophius piscatorius

ABSTRACT

The incorporation of trace elements into the calcified structures of fish can vary seasonally. Interpretation of these seasonal signals can provide information about fish age. This approach offers great promise for objectively estimating age and corroborating other methods of age estimation for fish stock assessment. This study investigated seasonal variation in trace element composition of otoliths and illicia from white anglerfish (*Lophius piscatorius* L.), a species that is very difficult to age using visual interpretation of growth bands in their calcified structures. A suite of trace elements (Na, Mg, Zn, Sr, Ba in illicia and Na, Mg, K, Sr, Ba in otoliths) was measured with LA-ICPMS using discrete ablations and continuous line scans. A method is presented to obtain reliable measurements of microchemical composition from illicia. Variation in elemental concentrations at the edge of the illicium was primarily related to fish length and no differences were detected between fish collected at different times of the year. In otoliths, Sr concentrations at the edge (0–100 μm) were highest in anglerfish collected during wintertime (quarter 1). Seasonal differences in Sr were statistically significant but small; a larger proportion of the explained variance was attributed to length and individual variability. Nonetheless, the seasonal pattern was consistently detected across all size classes, indicating that the analysis of cycles in otolith Sr could potentially provide a tool to support age estimation in white anglerfish.

1. Introduction

A robust understanding of life history strategies and growth dynamics supports the effective management of fishes in marine, coastal and freshwater systems worldwide. Calcified structures such as otoliths, bones and scales, register the individual history of each fish, with the daily and seasonal growth patterns recorded in the structure of the organic and inorganic matrix as visual growth marks. Moreover, the chemical composition of calcified structures record environmental variations and physiological responses that may allow the identification of origin, tracking of migrations, reconstruction of environmental history, measurement of age and assessment of diet (Gillanders, 2005; Hüssy et al., 2020; Walther, 2019). For instance, seasonal changes in temperature and physiology can produce periodic patterns in the chemical composition of otoliths (Seyama et al., 1991). Across several species, clearly defined minima and maxima in the concentrations of some elements and isotopes have been shown to correspond to age (Heimbrand et al., 2020; Hüssy et al., 2015; Kastelle et al., 2017; Siskey et al., 2016). These patterns provide a tool to validate the periodicity of growth marks in calcified structures. The approach is particularly useful for stocks without clearly defined, annually recurring growth marks in their calcified structures, an issue that can hamper age estimation and age-based assessment and challenge the implementation of Maximum Sustainable Yield (MSY)-based management, as is required under the common fisheries policy (CFP) (Maunder and Piner, 2014).

The white anglerfish (*Lophius piscatorius* Linnaeus, 1758) provides an interesting case study for developing microchemistry-based approaches to age validation. White anglerfish is a bottom-living species that occurs

* Corresponding author.
E-mail address: deirdre.brophy@gmit.ie (D. Brophy).

https://doi.org/10.1016/j.ecss.2021.107557
Received 3 February 2021; Received in revised form 1 July 2021; Accepted 15 August 2021
Available online 30 August 2021

from shallow, inshore waters to deeper than 1000 m (Quéro and Vayne, 2005; Whitehead et al., 1986). In Europe, the species has high commercial value and is caught together with black anglerfish (*Lophius budegassa*) by trawl and gillnetting fleets (Fariña et al., 2004); in recent years catches of the two species have exceeded 60,000 t yr^{-1} (FAO, 2019). Available age-estimation methods for white anglerfish have low reliability. The occurrence of secondary structures makes age estimation using otoliths difficult (Crozier, 1989; Woodroffe et al., 2003). As a consequence, the illicium (the modified first spine of the dorsal fin, which acts as a lure) is the preferred structure for routine age estimation in most European countries (ICES, 2011; Landa et al., 2008). The periodicity of growth marks in illicia has been indirectly validated using length cohort analysis. However, uncertainties remain regarding interpretation of growth marks in both ageing structures (Velasco et al., 2008; Wright et al., 2002). There are large inconsistencies between age estimates obtained from otoliths and illicia and considerable disagreement between readers interpreting the same structures (ICES, 2011; Woodroffe et al., 2003). Moreover, white anglerfish tagging studies show that counting of visual bands on illicia leads to over-estimation of age, largely due to misinterpretation of the first winter ring (Landa et al., 2008). Direct estimates of age are therefore considered unreliable and are not used in stock assessment for any of the anglerfish stocks in the Northeast Atlantic. Assessments are instead based on survey indices or length-based methods (ICES, 2018). A reliable method of age determination would help to validate the growth models used in the assessments and could improve the estimation of MSY reference points.

For species that are difficult to age from visual examination of their growth structures, methods based on microchemistry of their calcified structures offer great promise for objectively estimating age and corroborating other methods of age estimation. The primary objectives of this study were to analyse microchemistry patterns in anglerfish otoliths and illicia, to establish if elements show seasonal variation, and to evaluate the potential use of seasonal patterns in composition for validating or verifiying age estimates. While numerous studies deal with age-related trends in otoliths (Heimbrand et al., 2020; Hüssy et al., 2015; Kalish, 1991; Morales-Nin et al., 2014; Tomas et al., 2006; Tzeng et al., 1999), only a few have examined these patterns in fin spines such as illicia or dorsal spines. Differences in microchemistry between opaque and translucent bands have been detected in bluefin tuna (Luque et al., 2017); albacore tuna (Davies et al., 2011) and sturgeon (Jaric et al., 2011). A secondary objective of this study was therefore to establish a protocol for the reliable detection of seasonal trends in illicia sections. In order for chemical constituents of otoliths or illicia to provide a reliable indicator of age, their deposition must follow a regular seasonal cycle that is reasonably consistent across age groups, sexes and geographic areas. Here, the seasonality of microchemistry patterns was tested by comparing the composition at the edge of each structure between fish collected at different times of year.

2. Material and methods

2.1. Sample collection

Samples of anglerfish were collected in 2017 and 2018 from ICES area 7 during scientific surveys on board RV Celtic Explorer and from port samples taken by the Marine Institute and Ifremer (Fig. 1). From the available material, samples were selected to represent the four quarters of the year (Q1 = January–March, Q2 = April–June, Q3 = July–September, Q4 = October–December) and from four size categories: < 31 cm total length (TL), 31–41 cm TL, 42–52 cm TL, > 52 cm TL. The first three size categories were chosen to represent the main length cohorts in the stock as indicated by the length cohort analysis of Batts et al. (2019). The larger fish were included even though they are less abundant, because age estimates are particularly difficult for individuals in this size class (Hans Gerritsen pers. obs.). One sagittal otolith and the illicium were removed from each individual and stored separately in plastic tubes.

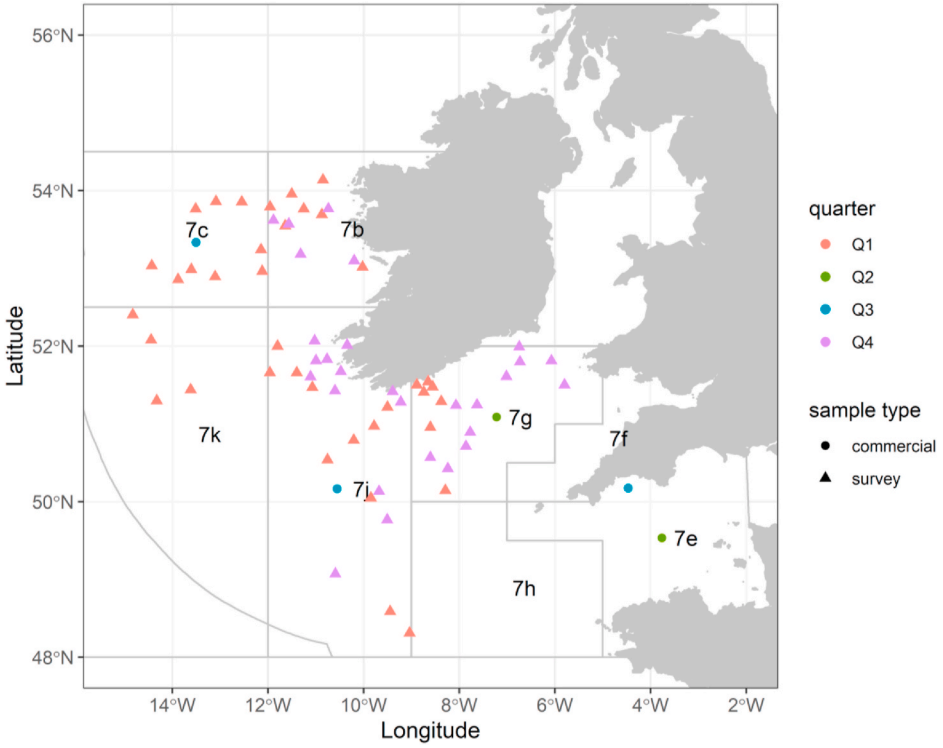

Fig. 1. Sampling locations of anglerfish selected for analysis of otolith and illicia elemental concentrations. Symbols represent the method of collection (circles = commercial fishery, triangles = scientific survey). Colours indicate the season of collection (orange = Q1, green = Q2, blue = Q3, purple = Q4). (For interpretation of the references to colour in this figure legend, the reader is referred to the Web version of this article.)

2.2. Study design

The microchemistry analysis was conducted in two phases. In the pilot phase, 20 otoliths and 20 illicia (10 fish collected in quarter 3, 2017 and 10 from quarter 1, 2018) were analysed for a range of trace elements to determine which showed the most variation between fish collected in different seasons. In the main phase, the otoliths from 127 anglerfish collected in quarter 4 in 2017 and in quarters 1, 2 and 3 in 2018 were analysed for the trace elements that showed the strongest seasonal signals in the pilot phase (Table 1).

2.3. Calcified tissues preparation

Sagittal otoliths and illicia were soaked in deionised water for 5–10 min to remove any biological tissue. Otoliths were mounted in epoxy resin (Buehler EpoThin2), and ground on the sagittal plane (sulcus side) with P320 and P1500 to P4000 grit silicon carbide paper to expose the otolith surface and to produce a flat sagittal section. Final polishing was conducted using diamond suspensions (9 μm, 3 μm and 1 μm) and sections were glued using a thermolabile resin (Crystalbond) in randomised positions onto petrographic glass slides.

Illicia were mounted in polyester resin (Crystic R115PAV01) and sectioned transversally according to the protocol described by Duarte et al. (2002). Three sections of between 0.3 and 0.5 mm thickness were taken from the base of each illicium. Sections were ground with P2500 to P4000 sanding papers, polished using diamond suspensions (3 μm and 1 μm) and then glued using Crystalbond to petrographic glass slides in randomised positions.

Prior to analysis, all the preparations were decontaminated by sonication in MilliQ water for 1 min, followed by soaking in 5% HNO_3 Suprapur for 15 s, triple rinsing in MilliQ water, and final sonication in a MilliQ bath for 1 min. They were then allowed to dry for 24 h in a laminar flow hood and stored in double zip plastic bags.

2.4. Preliminary assessment of the composition of the illicium

Unlike otoliths, which are predominately composed of calcium carbonate crystallized as aragonite, teleost fin rays and spines are composed of dermal bone, consisting primarily of calcium phosphate in the form of hydroxyapatite ($Ca_{10}(PO_4)_6(OH)_2$) (Ugarte et al., 2011). Differences in structure and composition between illicia and otoliths will affect how elements and isotopes are incorporated and have consequences for the analytical protocols used to analyse illicia (e.g. choice of method and standards, limits of detection, range of elements/isotopes analysed). Therefore, preliminary analyses were conducted to develop the optimal protocol for the illicia analysis, whereas otolith methodologies were based on previous protocols (Catalán et al., 2018; Morales-Nin et al., 2014).

Laser-Ablation Inductively Coupled Plasma Mass Spectrometry (LA-ICPMS) was the surface-based analytical technique selected to quantify the chemical composition of both otoliths and illicia. A review of the literature using Web of Science was conducted to collate information pertaining to the analysis of illicia using LA-ICPMS (Table 1, Supplementary Material, references cited therin: Allen et al., 2009; Arai et al., 2002; Clarke et al., 2007; Davies et al., 2011; Feldlite et al., 2008; Gillanders, 2001; Kennedy et al., 2000; Köck et al., 1996; Luque et al., 2017; Phelps et al., 2012; Pollard et al., 1999; Rude et al., 2014; Scharer et al., 2012; Smith and Whitledge, 2010, 2011; Tillett et al., 2011; Ugarte et al., 2012; Vas, 1991; Veinott et al., 1999; Wolff et al., 2013. Elements that tend to display potentially age-related trends in fin spines and vertebrae were identified: Sr, Zn, Ba, Mn and Cu. This list is similar to the suite of elements that have proved useful for age validation using otolith microchemistry (Heimbrand et al., 2020; Hüssy et al., 2015; Siskey et al., 2016).

A preliminary microchemical analysis was performed in four anglerfish illicia using a Hitachi S3400N SEM with a Bruker ACS XFlash 4010 detector at Universitat de les Illes Balears. The purpose of the analysis by energy dispersive X-ray spectroscopy (EDS) was to qualitatively characterise the chemical composition of the illicia and the resin used for embedding the structure and to identify potential contamination issues due to sample preparation. SEM was used in backscattered mode on 150 × 100 μm surface samplings in both illicia and surrounding resin. Spectra for C, O, F, Na, Mg, P, Ca, Cl, S and K were qualitatively obtained. The results showed that the composition of the resin was very different from that of the illicia and the two materials are easily distinguished (Fig. 1, Supplementary Material). Resin did not penetrate the illicium.

Due to the small size of illicia (mean diameter 0.85 mm) and the need for a good signal for LA-ICPMS analysis, three laser beam diameters (10 μm, 25 μm, 40 μm) were tested to obtain the optimal balance between response analysis and spatial resolution. The comparison of the different spot sizes showed unreliable signals for spot sizes of 10 μm. Isotope profiles for spots of 25 μm and 40 μm size were both stable and properly quantified, with scans of 40 μm providing the higher signal intensities but lower spatial resolution. The results showed that the spot size of 25 μm was optimal in terms of accuracy and spatial resolution (Fig. 2, Supplementary Material). In the subsequent analysis, data were collected from illicia using both 25 μm diameter spot analyses and continuous line scans of 25 μm wide.

2.5. Laser-ablation ICPMS analysis

The LA-ICPMS analysis of anglerfish otoliths and illicia was carried out at the Universidade de A Coruña using a CETAC Laser Ablation System LSX-213 G2+ coupled to a Thermo-Finnigan ICPMS Element XR. During the pilot phase, a series of spot ablations of 40 μm diameter, with 70 μm spacing (otoliths) and 25 μm diameter with 40 μm spacing (illicia) were made on each section. Complete core to edge transects were analysed on the illicia, while on each otolith, a section at the edge corresponding to recent growth (at least 280 μm long) was analysed. Additionally, continuous line scans were made on the illicia sections from the core outward to the edge (25 μm width); on the otoliths the line scans were taken from the edge towards the core for a distance of at least 1250 μm (40 μm width). In the main phase, continuous line scans (40 μm width) were taken from the core to the edge of each otolith section (Fig. 2). The scan speed of all continuous line scans was 10 μm s^{-1}.

The reference standards used in the analysis of both otoliths and illicia were the glass standards: NIST612, NIST614 and NIST616.

Table 1
Number of anglerfish samples from each size category and quarter that were included in the pilot phase and main phase of the analysis.

Quarter	Year	Size category (cm)							
		<31		31–41		42–52		>52	
		pilot	*main*	*pilot*	*main*	*pilot*	*main*	*pilot*	*main*
1	2018		10	2	10	2	9	6	6
2	2018		9		9		9		4
3	2017			1		4		5	
3	2018		3		11		10		7
4	2017		9		9		8		4

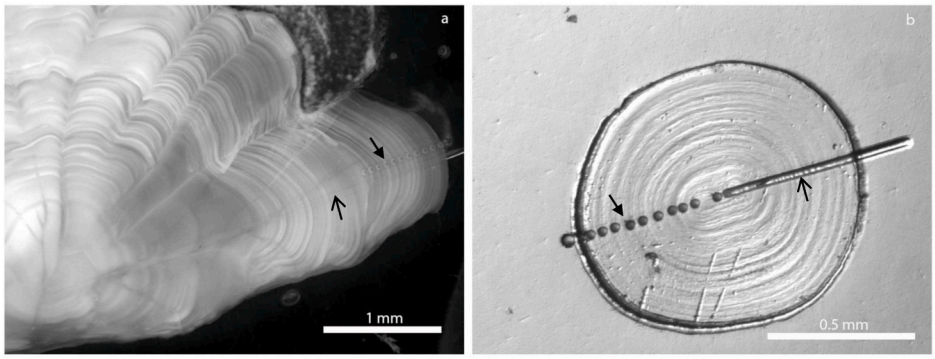

Fig. 2. Anglerfish otolith (a) and illicium (b) thin sections showing core-to-edge spot transects (closed head arrow) and continuous laser ablation-lines (open head arrow). Scan width sizes are 40 μm for otoliths and 25 μm for illicia.

Additionally, due to the different composition of bone and otoliths, a specific bone meal standard (NIST1486) pressed as a pellet was used in the analysis of the illicia; whereas FEBS-1 (Sturgeon et al., 2005) and NIES-22 (Yoshinaga et al., 2000) pressed as pellets were used for the otoliths. All reference materials were ablated following the bracketing procedure, being measured at the beginning and end of each working session and every five scans on the calcified structures. In the pilot phase, a suite of elements was initially quantified: ^{7}Li, ^{23}Na, ^{24}Mg, ^{26}Mg, ^{27}Al, ^{31}P, ^{39}K, ^{43}Ca, ^{44}Ca, ^{55}Mn, ^{56}Fe, ^{66}Zn, ^{88}Sr, ^{137}Ba, ^{138}Ba, ^{206}Pb, ^{207}Pb and ^{208}Pb. Elements with low accuracy (<90% or >110%) or poor recovery (relative standard deviation > 10%) were rejected from subsequent analysis. For the illicia line scan and spot analyses, ^{23}Na, ^{66}Zn, ^{88}Sr and ^{138}Ba were retained; for the illicia spots ^{24}Mg was also included. For the the otoliths, ^{23}Na, ^{24}Mg, ^{26}Mg,^{39}K, ^{88}Sr and ^{138}Ba could be reliably measured in spots and line scans and data for these elements were retained for analysis.

In LA-ICPMS analysis, variability in the elemental signals can arise due to elemental fractionation, matrix effects and variation in ablation yield (Günther et al., 1999). To correct for this, an element that is present at a known concentration within the sample can be used as an internal standard. Calcium is present in both otoliths and illicia at a reasonably consistent concentration, thus a value of 38.8 wt% (Yoshinaga et al., 2000) of ^{43}Ca in otoliths and 26.0 wt% (Veinott and Evans, 1999) of ^{43}Ca in illicia was used as internal standard. The raw data were processed using software Iolite (Melbourne University, Melbourne), a semiautomatic program for LA-ICPMS data reduction and calculation of isotope concentrations.

2.6. Statistical analysis

To test for seasonality of otolith microchemistry patterns, concentrations of elements and isotopes at the edge of the otoliths and illicia were compared between samples collected at different time points within an annual cycle (pilot phase: quarter 3, 2017-quarter 1, 2018; main phase: quarter 4, 2017, quarters 1, 2 and 3, 2018).

Elemental concentrations from the continuous line scans were expressed as 10 point moving averages. To control for innate variability in elemental concentrations between individuals, prior to analysis each data point on a given spot transect or line scan was divided by the mean elemental concentration on that transect to produce a mean standardised elemental concentration.

For the illicia spot transects, mean standardised elemental concentrations (E) at the spot closet to the edge of the structure were analysed using general linear models (GLMs) with quarter (Q) and length category (LC) included as factors in the analysis (equation 1). For the otolith spot transects, data were available at a finer temporal scale due to the larger size of the otoliths compared to the illicia. Therefore, the 3 spots closest to the edge were used to represent the season of capture. Elemental concentrations were analysed using general linear mixed models (GLMMs), with quarter and length category included as fixed effects and fish ID (ID) included as a random effect to account for the non-independence of multiple measurements from the same individual (equation 2). For the continuous line scans, elemental concentrations close to the edge (50 μm from edge for illicia, 100 μm for otoliths) were also analysed using GLMMs, as above (equation 2). In each case the full models were compared to a series of less complex models and to the null model (equation 3 for GLMs and eqation 4 for GLMMs) using Akaike information criterion (AIC) and log likelihood tests.

$$E = Q^{*}LC + \varepsilon \quad (1)$$

$$E = Q * LC + 1|\, ID + \varepsilon \quad (2)$$

$$E = 1 + \varepsilon \quad (3)$$

$$E = 1|\, ID + \varepsilon \quad (4)$$

Where patterns indicating that model residuals were not normally distributed were detected, the response variable was transformed using Box-Cox transformation.

In addition to size-related trends, otolith elemental concentrations may vary geographically. The sampling area was divided into three broad geographic regions: the northwest of the study area (ICES areas 7b-c), the south east of the study area (ICES areas 7e-f), and the centre of the study area (ICES areas 7g, j & k). When seasonal variation in elemental composition at the edge of the calcified structures was observed, potential confounding effects of spatial variability were investigated by examining seasonal differences in edge chemistry within regions using box plots and GLMs. Seasonal variation in standardized elemental concentrations along transects within each individual was also investigated. First, the portion of each otolith transect corresponding to the three months (0.25 year) prior to capture was extracted for each individual. To accomplish this, otolith growth rate was calculated from the total otolith radius based on the otolith size-fish size relationship (Fig. 3., Supplementary Material) and the body proportional back-calculation approach (Francis, 1990). Distances along the otolith radius were fitted to an estimated anglerfish von Bertlanffy growth model (Batts et al., 2019). Seasonal variation in body and otolith growth rate was accounted for using the approach of Somers (1988) to incorporate a sinusoidal function into the von Bertlanffy growth model; growth was assumed to reduce by 30% during winter, with the reduction starting in October. The transect length representing the final three months (0.25 year) of otolith growth was calculated, expressed as a proportion of the total radius, and the elemental concentrations were extracted for this portion of the line scan (Fig. 3). While this approach did not account for individual variability in the length-age relationship, it did correct for the substantial size-related variability in the length of the recent growth transect, for which estimates ranged from 64 μm for a 104 cm fish to 495 μm for an 8 cm fish.

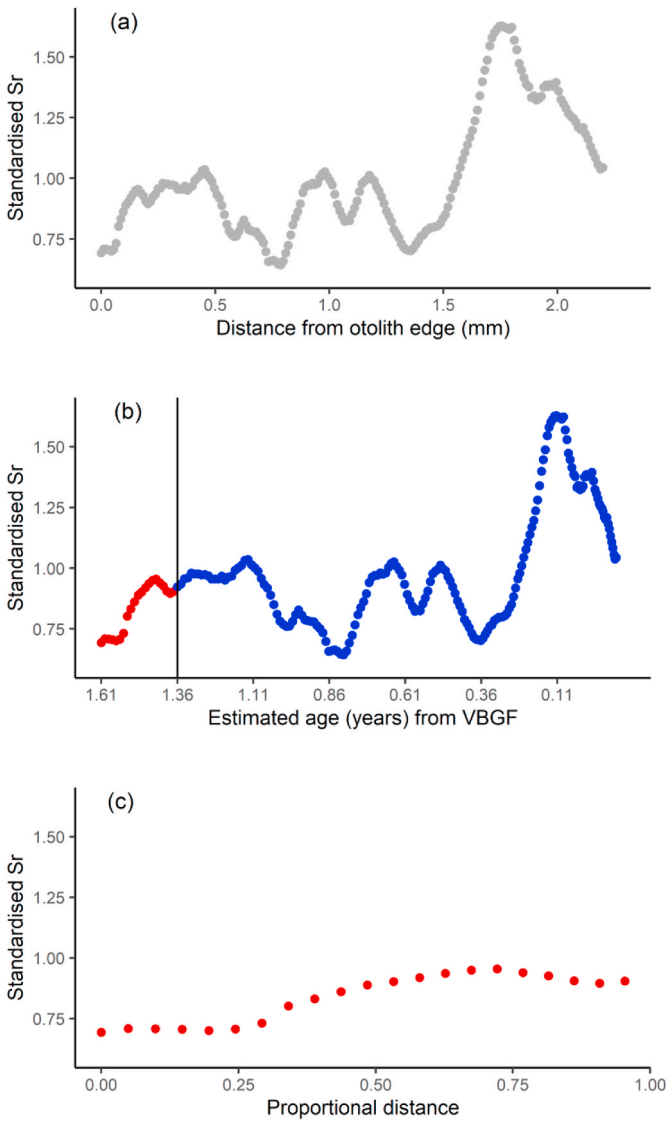

Fig. 3. Illustration of the procedure for extracting the portion of the transect corresponding to the previous three months of growth. Example is from an individual collected in quarter 2. The plots show the relationships between mean standardised Sr concentration (calculated by dividing each Sr measurement by the mean of all the Sr measurements from that transect) and (a) distance from the otolith edge; (b) estimated back-calculated age at each point on the same transect using the Von Bertalanffy growth function (VBGF), based on the model of Batts et al. (2019) and (c) the proportional distance along the recent growth transect (time of capture = 0; ~3 months prior to capture = 1). The vertical line in (b) separates data from the most recent 3 months of growth (red points) from the rest of the transect (blue points) based on the back-calculated age estimates. Plot (c) shows only the data from the most recent ~3 months of growth. (For interpretation of the references to colour in this figure legend, the reader is referred to the Web version of this article.)

It was predicted that if the concentration of an element in the otolith varied seasonally this would be reflected in the slope of the relationship between elemental concentration and proportional distance along the recent (~3 month) growth transect in samples from each quarter. A series of GLMMs was used to test this; mean standardised elemental concentrations were modelled as a function of proportional distance along the recent growth transect (D), with quarter included as a fixed effect, total fish length (L) as a covariate and fish ID (ID) as a random effect (equation 5).

$$E = D * Q + L + +1|\, ID + \varepsilon \quad (5)$$

For the GLMM's, the marginal R squared value provided a measure of the variance explained by the fixed effects while the conditional R squared value provided a measure of the total variance explained by the fixed and random effects combined (Morrongiello and Thresher, 2014; Nakagawa and Schielzeth, 2013).

All analyses were conducted in the R programming environment using R version 4.0.2 (R Core Team, 2020). GLMM models were run using the lme4 package (Bates et al., 2015) and the lmtest package (Zeileis and Hothorn, 2002) was used for likelihood ratio testing. Significance testing was conducted using the Lmertest (Kuznetsova et al., 2017) and emmeans (Lenth, 2020) packages. Plots were created using ggplot2 (Wickham, 2016).

3. Results

The results from the GLM and GLMM analyses of elemental concentrations in otoliths and illicia from the pilot and main phase of the investigation are summarised in Table 2.

3.1. Pilot phase analysis

3.1.1. Illicia

GLM analysis of the spot data from 20 illicia showed that mean standardised concentrations of Zn and Sr at the illicium edge varied significantly between fish of different size (Table 2, models 3 and 4; likelihood ratio test: $p = 0.02$ and $p = 0.03$ respectively), with no evidence of seasonal variation. For Ba, the best fitting model contained the quarter * length category interaction (Table 2, model 5; likelihood ratio test; $p = 0.003$) showing that seasonal variation was not consistent between length categories. Ba concentrations at the illicium edge were significantly higher in Q1 compared to Q3 for fish in the 31–41 cm length category ($p = 0.01$), but not for fish in the 42–52 cm or >52 cm length category ($p = 0.14$ and $p = 0.05$ respectively). For Na the model with the lowest AIC value included length category as a fixed effect, however, the likelihood ratio test found that this model did not provide a significantly better fit to the data compared to the null model, indicating that the length effect was not significant (Table 2, model 1; likelihood ratio test; $p = 0.07$). In the case of Mg, there was no evidence of variation between length categories or seasons (Table 2, model 2; likelihood ratio tests; $p > 0.05$).

GLMM analysis of the continuous line scan data from the 20 illicia showed that variability in mean standardised Zn, Sr and Ba was best explained by length category (Table 2, models 7, 8 and 9; likelihood ratio test: $p = 0.01$, $p = 0.02$ and $p = 0.01$ respectively), with no evidence of seasonal variability (likelihood ratio tests: $p > 0.05$). For Na, the model with the lowest AIC value included quarter as a fixed effect, however, this model did not provide a significantly better fit to the data compared to the null model, indicating that the variation between quarters was not significant (Table 2, model 6; likelihood ratio test: $p = 0.06$). Due to the lack of consistent seasonal differences in elemental concentrations, the analysis of illicia was not included in the main phase.

3.1.2. Otoliths

GLMM analysis of the spot data from 20 otoliths showed that variability in mean standardised ^{24}Mg and K was best explained by length category, with no evidence of seasonal variability (Table 2, models 11 and 13; likelihood ratio test; $p = 0.003$ and $p = 0.03$ respectively). For ^{26}Mg, the model with the lowest AIC value also included length category, but the fit was not significantly better than the null model (Table 2, model 12; likelihood ratio test: $p = 0.11$). For Na and Ba the best fitting model contained the quarter * length category interaction showing that seasonal variation was not consistent between length categories (Table 2, models 10 and 15; likelihood ratio test; $p = 0.008$ and $p = 0.04$ respectively). Na concentrations at the otolith edge were significantly higher in Q1 compared to Q3 for fish in the >52 cm length category ($p =$

Table 2
Model selection results for the GLM and GLMM analyses of elemental concentrations at the edges of otoliths and illicia. Statistically significant model fits, as determined by likelihood ratio tests (LR test) are highlighted in bold. For GLM models the variance explained by the model is expressed as the adjusted (Adj.) R^2. For GLMMs the marginal (Marg.) R^2 is the variance explained by the fixed effects while the conditional (Cond.) $R^2$is the variance explained by the fixed and random effects combined.

Dataset	Element	Model with lowest AIC value *(model reference number in brackets)*	Null model comparison		Adj. R^2	Marg. R^2	Cond. R^2
			Δ AIC	*p (LR test)*			
Illicia spot transects	^{23}Na	~ length category *(1)*	1.5	0.07	0.16		
Pilot phase	^{24}Mg	~1[a] *(2)*	_	_	_		
	^{66}Zn	**~length category** *(3)*	3.5	0.02	0.24		
	^{88}Sr	**~ length category** *(4)*	2.8	0.03	0.21		
	^{138}Ba	**~quarter*length** *(5)*	8.3	0.003	0.47		
Illicia line scans	^{23}Na	~quarter+(1|fish.ID) *(6)*	1.5	0.06		0.12	0.71
Pilot phase	^{24}Mg	*Insufficient data*					
	^{66}Zn	**~length category + (1|fish.ID)** *(7)*	4.5	0.01		0.23	0.64
	^{88}Sr	**~ length category + (1|fish.ID)** *(8)*	3.9	0.02		0.27	0.83
	^{138}Ba	**~ length category + (1|fish.ID)** *(9)*	5.0	0.01		0.31	0.78
Otolith spot transects	^{23}Na	**~quarter*length category + (1|fish.ID)** *(10)*	5.7	0.008		0.24	0.24
Pilot phase	^{24}Mg	**~length category + (1|fish.ID)** *(11)*	7.5	0.003		0.17	0.17
	^{26}Mg	~length category+(1|fish.ID) *(12)*	0.4	0.11		0.07	0.07
	^{39}K	**~length category + (1|fish.ID)** *(13)*	3.1	0.03		0.13	0.19
	^{88}Sr	~(1|fish.ID)[a] *(14)*					
	^{138}Ba	**quarter*length category + (1|fish.ID)** *(15)*	1.5	0.04		0.19	0.28
Otolith line scans	^{23}Na	~(1|fish.ID)[a] *(16)*	_	_		—	
Pilot phase	^{24}Mg	~length category+(1|fish.ID) *(17)*	0.8	0.10		0.13	0.66
	^{26}Mg	~length category+(1|fish.ID) *(18)*	1.8	0.06		0.18	0.71
	^{39}K	~(1|fish.ID)[a] *(19)*					
	^{88}Sr	**~quarter + (1|fish.ID)** *(20)*	4.3	0.01		0.23	0.86
	^{138}Ba	**~length category + (1|fish.ID)** *(21)*	4.9	0.01		0.29	0.83
Otolith line scans main phase (edge)	^{88}Sr	**~quarter + length category + (1|fish.ID)** *(22)*	35.4	<0.0001		0.28	0.93
Otolith line scans main phase (recent growth transect)	^{88}Sr	**~quarter*distance + length + (1|fish.ID)** *(23)*	122.4	<0.0001		0.13	0.50
		~quarter*distance+(1|fish.ID) *(24)*	96.0	<0.0001		0.06	0.52

[a] The null model.

0.004), but not for fish in the 31–41 cm or 42–52 cm length category (p = 0.40 and p = 0.27 respectively). In the case of Ba, concentrations at the otolith edge were significantly higher in Q1 compared to Q3 for fish in the 31–41 cm length category (p = 0.002), but not for fish in the 42–52 cm or >52 cm length category (p = 0.59 and p = 0.77 respectively). Mean standardised Sr concentrations of otolith edge spots did not vary between quarters or length categories (Table 2, model 14; likelihood ratio tests: p > 0.05). However, GLMM analysis of the line scan data from the 20 otoliths revealed a significant seasonal effect (Table 2, model 20; likelihood ratio test: p = 0.01). The analysis of the otolith line scan data also indicated that Ba at the otolith edge varied between length categories but not quarters (Table 2, model 21;

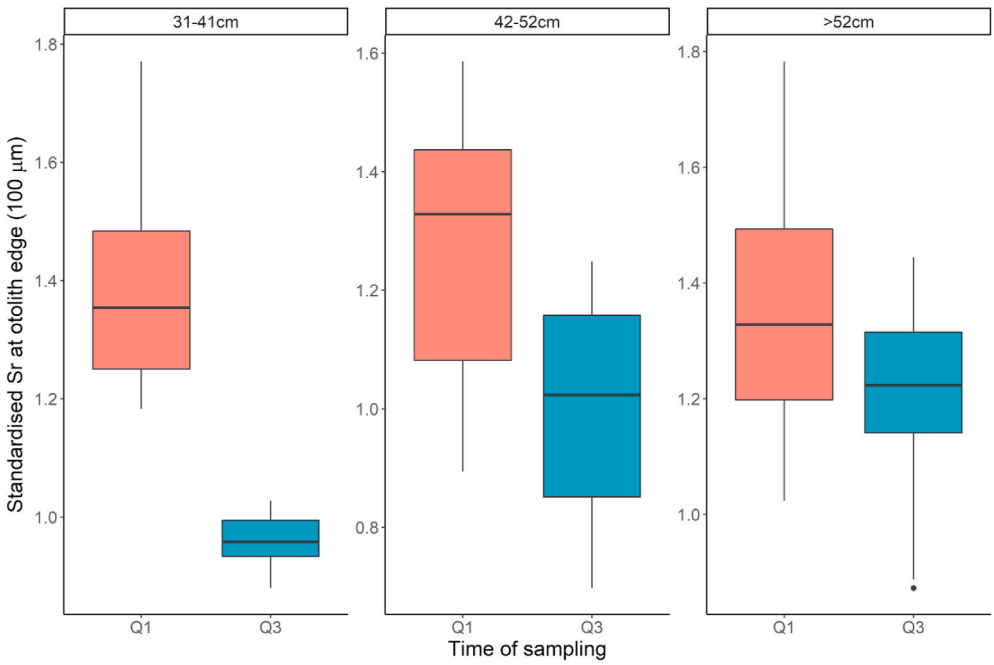

Fig. 4. Seasonal and size-dependent differences in mean standardised concentrations of Sr in the outermost area of otoliths (0–100 µm from the edge). Plots show the results of pilot phase analysis using LA-ICPMS continuous line scans, and compare fish in different length categories, sampled in different quarters. Mean standardised Sr concentrations were calculated by dividing each Sr measurement by the mean of all the Sr measurements from that transect.

likelihood ratio test: $p = 0.01$). AIC values indicated that models containing length category provided the best fit to the Mg data, however the fit was not significantly better than the null model (Table 2, models 17 and 18; likelihood ratio test: $p = 0.1$ and $p = 0.06$ for ^{24}Mg and ^{26}Mg respectively). Mean standardised concentrations of K along otolith line scans did not vary between length categories or quarters (Table 2, model 19, likelihood ratio tests: $p > 0.05$).

Overall, the pilot phase analysis found that Sr from otolith line scans showed the strongest seasonal signals. The addition of the length category * quarter interaction did not improve the model fit, indicating that seasonal differences in Sr were largely consistent across length categories. However, visual inspection of the data indicated that the magnitude of the difference decreased with fish size (Fig. 4). Mean standardised concentrations of Sr at the otolith edge were higher in samples collected in Q1 compared to Q3. The main phase analysis was therefore focussed on further analysis of seasonal variability in Sr at the otolith edge across Q1-Q4.

3.2. Main phase analysis

Mean standardised Sr concentrations measured along lines scans on 127 otoliths were analysed using GLMMs. The best fitting model included quarter and length category, but not the interaction, (Table 2, model 22). Both quarter and length category were statistically significant ($p = 0.006$ and $p < 0.0001$ respectively). Sr concentrations at the otolith edge (0–100 μm) were highest in Q1 followed by Q4 and Q3. The lowest concentrations were observed in Q2 (Fig. 5). Tukey post-hoc tests confirmed that the difference between Q1 and Q2 was statistically significant ($p = 0.005$). None of the other pairwise comparisons were significant ($p > 0.05$, Table 3).

Sr concentrations at the otolith edge (0–100 μm) increased with fish size (Fig. 5). Tukey post-hoc tests confirmed that fish in the smallest size class (<30 cm) had significantly lower Sr concentrations at the otolith edge compared to all other size classes ($p < 0.01$). Fish in the largest length category (>52 cm) had significantly higher Sr concentrations at the otolith edge compared to fish in the 31–41 cm length category ($p = 0.02$; Table 3).

To investigate if the observed seasonal trends could be confounded by spatial variation in Sr concentrations across the sampling area, seasonal comparisons were plotted for three broad geographic regions (Fig. 6). These areas were: the northwest of the study area (ICES areas 7b-c), the south east of the study area (ICES areas 7e-f), and the centre of the study area (ICES areas 7g, j & k). Two of the regions were sampled in Q2 (7e-f and 7g, j & k). In both of these regions, Sr concentrations at the otolith edge were lower in Q2 compared to samples collected at other times of year. The difference was statistically significant for samples from ICES area 7e-f ($p = 0.00013$), but not for samples from ICES areas 7g, j & k ($p = 0.26$). In the analysis of the full dataset, including ICES area or region in the GLMM did not improve the model fit.

Within individuals, mean standardised Sr concentrations varied as a function of proportional distance from the otolith edge towards the core along recent growth transects (the three-month period prior to capture). The best fitting model included the interaction between proportional distance and quarter, the fish total length and fish *ID* as a random effect (Table 2, model 23). This confirmed that the slope of the relationship between elemental concentration and proportional distance varied between quarters (Fig. 7). Notably, the slope was positive in otoliths of anglerfish collected in Q2, indicating that mean standardised Sr concentrations increased from the edge (material deposited in Q2) to the end of the recent growth transect (material deposited three months previously). This is consistent with the results of the cross-individual comparison of otolith edge data (Table 3) which showed that mean standardised Sr concentrations were lowest in Q2. The consistency in the results of the within-individual and cross-individual comparisons indicates that the observed differences in Sr concentrations between anglerfish collected in different quarters are real seasonal effects, and not limited to a restricted portion of the geographical area sampled.

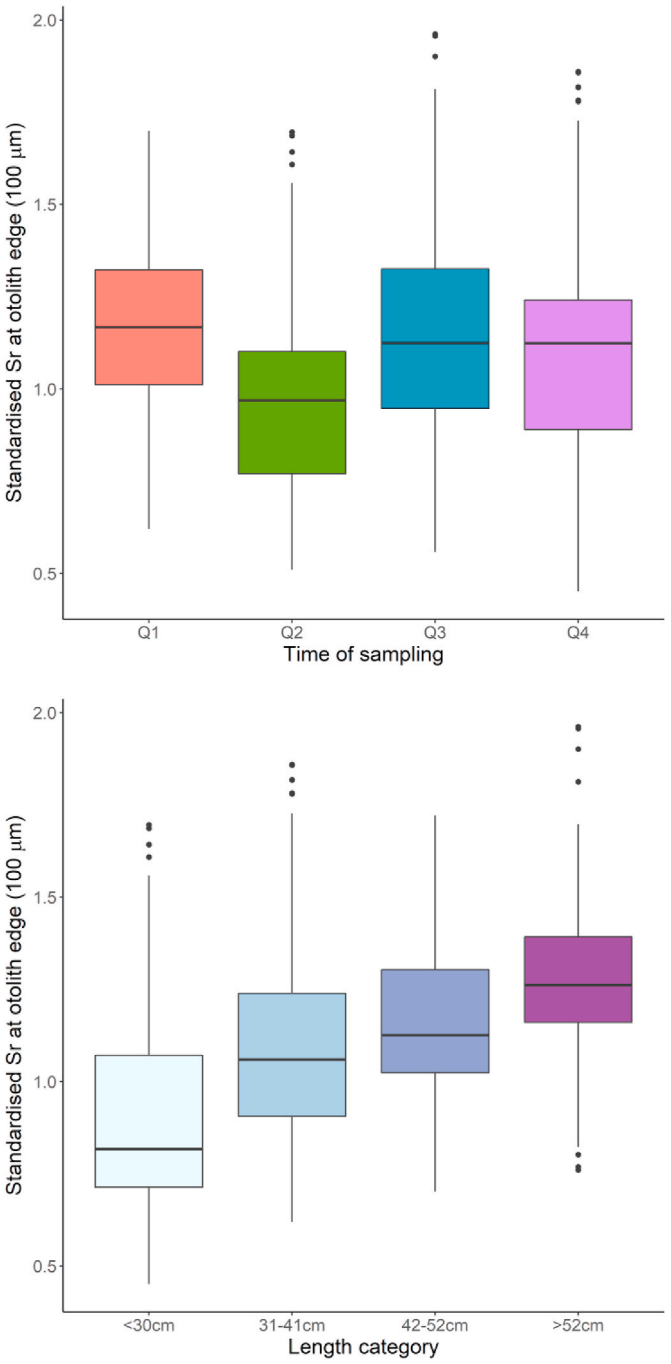

Fig. 5. Boxplots showing the variability in mean standardised concentrations of Sr in the otolith (0–100 μm from the edge) as detected in the main phase of the analysis using LA-ICPMS continuous line scans. Mean standardised Sr concentrations were calculated by dividing each Sr measurement from a given transect by the mean of all the Sr measurements from that transect.

Although significant ($p < 0.0001$), the seasonal trend indicated by the quarter * distance interaction was relatively minor, accounting for just 5.5% of the variation in Sr concentrations along recent growth transects (Table 2, model 24). A further 7.1% of the variance was explained by adding fish length (Table 2, model 23), while variation between individual fish (the $(1|ID)$ random effect) accounted for the largest proportion of the variance (37.4%).

Table 3
Pairwise comparisons of mean standardised Sr concentrations between quarters and length categories from the GLMM: Sr ~ quarter + length category+(1|fish.ID) and based on data from otolith line scans collected during the main phase.

Factor	Pairwise comparison	estimate	Standard error	df	t ratio	p value
Quarter	Q1 *vs* Q2	0.18	0.05	133	3.43	0.005
	Q1 *vs* Q3	0.06	0.05	133	1.13	0.670
	Q1 *vs* Q4	0.05	0.05	133	0.98	0.764
	Q2 *vs* Q3	−0.12	0.06	133	−2.15	0.14
	Q2 *vs* Q4	−0.13	0.05	133	−2.35	0.091
	Q3 *vs* Q4	−0.009	0.06	133	−0.16	0.998
Length category	<30 *vs* > 52	−0.3	0.06	133	−5.73	<0.0001
	<30 *vs* 31-41	−0.19	0.05	133	−3.65	0.002
	<30 *vs* 42-52	−0.28	0.05	133	−5.06	<0.0001
	>52 *vs* 31-41	0.17	0.06	133	2.91	0.022
	>52 *vs* 42-52	0.08	0.06	133	1.40	0.500
	31-41 *vs* 42-52	−0.08	0.05	133	−1.71	0.323

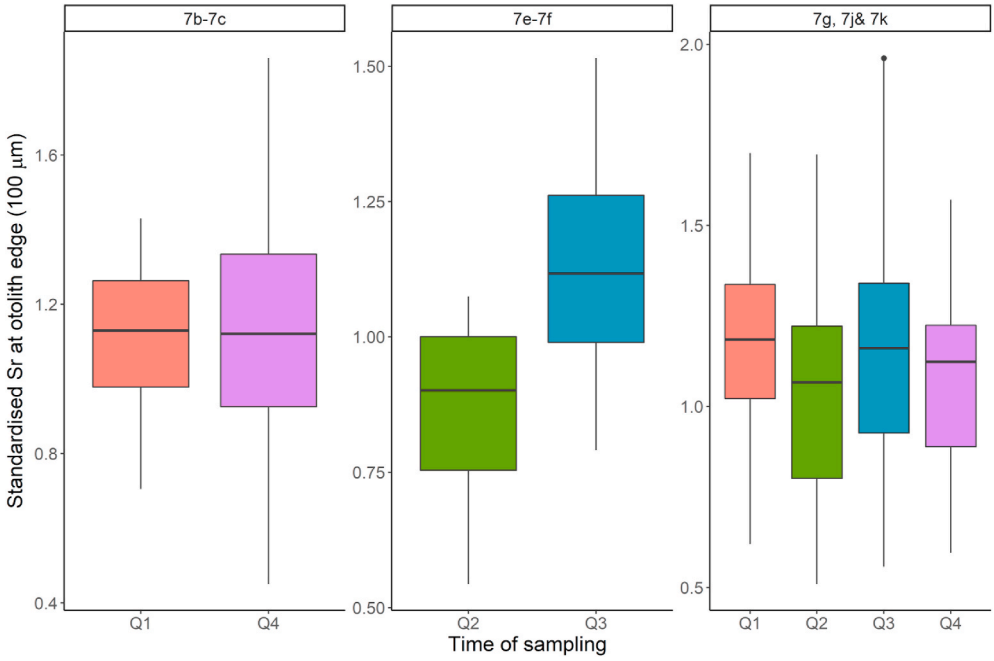

Fig. 6. Boxplots showing the variability in mean standardised concentrations of Sr in the otolith (0–100 µm from the edge) between quarters and areas, as detected in the main phase of the analysis using LA-ICPMS continuous line scans. See Fig. 1 for subarea location. Mean standardised Sr concentrations were calculated by dividing each Sr measurement from a given transect by the mean of all the Sr measurements from that transect.

4. Discussion

Trace element concentrations in calcified structures often vary across life history transects due to fluctuations in metabolism or environmental conditions (Kalish, 1991; Morales-Nin et al., 2012). Before these patterns can be used for age determination or to validate the use of visible growth patterns, it must first be established that they have a consistent seasonal basis (Vitale et al., 2019). This study investigated trace element concentrations at the edge of white anglerfish otoliths and illicia as an important first step in the development of microchemistry-based age determination methods for the species.

The illicium is the structure that is most widely used to estimate age in white anglerfish, although due to ambiguity in the interpretation of growth bands these estimates are not used in stock assessment (ICES, 2011; ICES, 2018; Landa et al., 2008). If clear seasonal patterns exist in the trace elemental composition of the illicia, these could be used to validate the annual nature of visual structures and to resolve discrepancies in their interpretation. Here, a protocol is presented for LA-ICPMS measurements from both discreet analysis spots and continuous line scan transects. Despite their small size and relatively porous structure, the illicium was not contaminated by resin impregnation during sample preparation. The results show that a range of trace elements can be reliably detected in illicia using LA-ICPMS.

The trace elemental concentrations at the edge of the illicium varied between fish length categories, but there were no statistically significant differences detected between fish collected in Q1 compared to Q3. The failure to detect a consistent seasonal signal may reflect the small size of the structure and the difficulty of isolating the most recent growth period. A 25 µm size analysis spot represents between 0.5 and 8 months of growth while the 50 µm line scan transect could capture between 1 and 15 months of growth. These estimates of spatial-temporal resolution depend on the age of the fish and are based on current growth models for white anglerfish (Batts et al., 2019; Landa et al., 2013) and the relationship between fish length and illicia diameter (Fig. 3, Supplementary material). It is likely that in larger fish the "edge" incorporated growth from several seasons, thereby diluting any difference in edge chemistry between fish captured at different times of the year. While the continuous line scan method can provide higher spatial resolution than discrete spot analyses in LA-ICPMS (Sanborn and Telmer, 2003), a higher spatial-temporal resolution could potentially be achieved using other approaches. For example, micro-PIXE and scanning X-ray fluorescence microscopy can be used to produce high resolution 2D

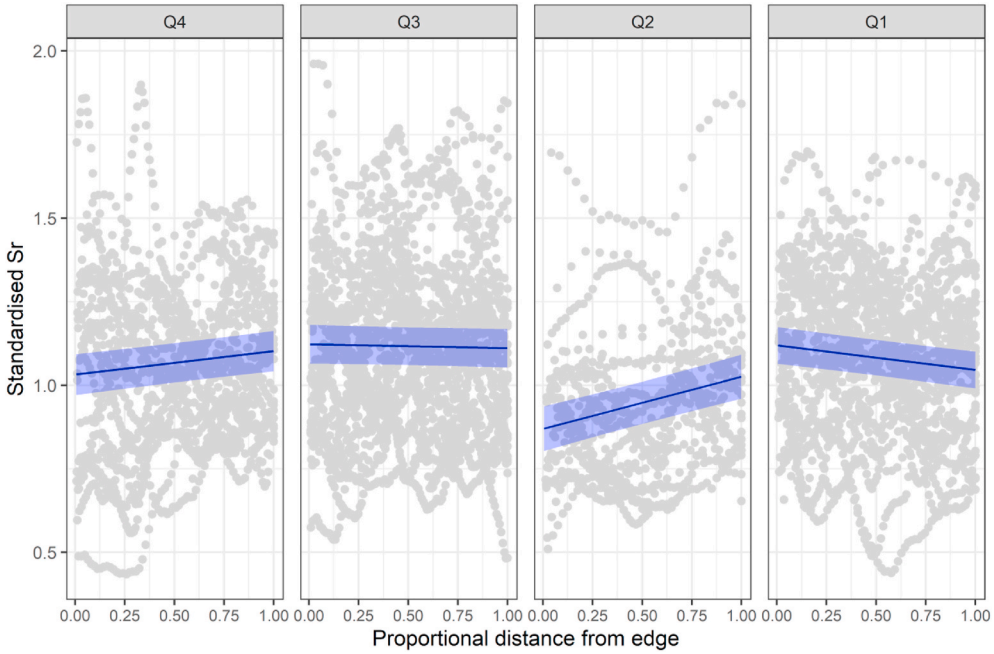

Fig. 7. GLMM output showing how mean standardised Sr concentration in the otolith changes along the recent growth transect, from time of capture to ~3 months prior to capture. Plot headings indicate the season of capture (Q1 = quarter 1; Q2 = quarter2; Q3 = quarter 3; Q4 = quarter 4). The X-axis represents the line scan transects, moving from the most recent otolith material at the otolith edge (axis value: 0) to material deposited ~3 months previously (axis value: 1). Mean standardised Sr concentrations were calculated by dividing each Sr measurement from a given transect by the mean of all the Sr measurements from that transect.

elemental maps down to a resolution of 5 μm and 15 μm respectively (Limburg and Elfman, 2017), which could allow for the detection of seasonal changes in the microchemical composition of illicia.

Analysis of the otoliths produced more promising results for identifying seasonal patterns in elemental concentration that could be applied to age estimation or validation. The strongest seasonal signal was detected in Sr measurements from the otolith line scans, which showed small but significant levels of variation in the material formed during recent otolith growth for individuals collected at different times of the year. Seasonal differences were overlaid on length-dependant variation in Sr. The relationship with length is not surprising; numerous studies report ontogenetic variation in otolith trace elements, including Sr (Macdonald et al., 2020; Morales-Nin et al., 2014; Sturrock et al., 2015). Crucially, in white anglerfish otoliths the seasonal pattern was consistently detected across all size classes. The results indicate that uptake of Sr into the otolith was highest during winter (Q1) and lowest during the spring and summer (Q3 in pilot phase, Q2 in main phase). There was some discrepancy between the pilot and main phase, which may be attributed to inter-annual variation in seasonal environmental patterns, geographic differences in seasonal microchemistry patterns or spatio-temporal variation in depth-occupancy behaviours (fish in deeper waters would not be exposed to the same temperature fluctuations). Nonetheless, the results indicate that Sr deposition in white anglerfish otoliths varies seasonally across length groups and is highest in winter.

Seasonal variation in Sr could reflect intra-annual changes in ambient water chemistry, fish physiology, or a combination of both. Strontium substitutes for calcium in the aragonite matrix of the otolith (Doubleday et al., 2014) at a rate that is generally proportional to ambient concentrations (Bath et al., 2000; Elsdon and Gillanders, 2005; Kraus and Secor, 2004; Reis-Santos et al., 2013; Walther and Thorrold, 2006) and varies with temperature (Bath et al., 2000; Elsdon and Gillanders, 2002; Reis-Santos et al., 2013; Townsend et al., 1992). Investigations of temperature dependence give conflicting results, and it is suggested that temperature indirectly affects otolith Sr via its influence on physiological processes (e.g. growth and reproduction) that determine blood plasma Sr levels (Sturrock et al., 2015). Several studies have shown that the rate of uptake of Sr into the otolith is relatively high during periods of slow growth (Miller and Hurst, 2020; Mugiya and Satoh, 1997; Sadovy and Severin, 1994; Sturrock et al., 2014; Walther et al., 2010). While in some species, otolith Sr maxima have been associated with maturation and reproduction (Clarke and Friedland, 2004; Granzotto et al., 2003). It is unlikely that the seasonal differences observed in this study are linked to reproduction as the variation in otolith Sr was evident in the smallest size class (<31 cm) which included immature individuals. It is more probable that the observed increase in Sr during winter and the decrease during spring/summer reflect seasonal changes in temperature and the growth rate of white anglerfish.

Within the study area, sea temperatures (0–110m) are relatively stable and low in Q1 and high in Q3, whereas temperatures increase during Q2 and decrease during Q4; in deeper waters (>110m) there is little seasonal fluctuation in temperature (Good et al., 2013), (Fig. 4, Supplementary Material). The white anglerfish is found from 50 to 1000 m depth (Whitehead et al., 1986), occupying progressively deeper waters with increasing size (Laurenson et al., 2005). In the Mediterranean, the highest probability of occurrence is between 200 m and 600 m depth (Barcala et al., 2019). Although it is a bottom dwelling species, occurrence in near-surface waters has been reported (Hislop et al., 2000), and an individual carrying a data storage tag was observed to make vertical migrations between the bottom and the surface (Thangstad et al., 2006). It is suggested that anglerfish may rise upwards into the pelagic zone to use selective tidal stream transport during migrations (Laurenson et al., 2005). Seasonal movements from inshore to offshore waters between November and April are also reported (Laurenson et al., 2005). Given their preference for deeper waters, anglerfish are generally not exposed to strong seasonal fluctuations in water temperatures. Intra-annual variation in temperature exposure and growth rates may be more strongly influenced by vertical and horizontal migrations, which can be extensive (Laurenson et al., 2005; Thangstad et al., 2006). Such variation may contribute to the observed seasonal patterns in otolith Sr. Future studies that combine otolith microchemistry and data storage tag profiles could help to reveal the underlying mechanisms.

The results confirm that seasonal variation in otolith Sr is detectable in white anglerfish across a wide geographic area and a range of length classes. With further development, microchemistry analysis could be used to support age determination and validation in white anglerfish, to corroborate interpretations of visual growth marks and to resolve discrepancies between estimates obtained from otoliths and illicia. Further work is needed to assess if the seasonal signal found in the otolith edge is present along the fish growth transect and to establish the extent to which microchemistry patterns correspond to visual growth marks. The

isolation of the relatively weak seasonal signal from length-based and individual variability presents a significant challenge that could be addressed using time series analysis approaches (e.g., detrending to remove ontogenetic effects) and signal processing methods. Otolith chemistry-based approaches have long been promoted as a direct validation method to support fish age determination and offer particular promise for difficult to age species (Heimbrand et al., 2020). These approaches rely on the identification of cyclical variation in elemental concentrations (Hüssy et al., 2015; Siskey et al., 2016) and the analysis of seasonal differences, as reported here. Alongside a growing understanding of the relationship between visible growth features and elemental composition (Granzotto et al., 2003; McFadden et al., 2016; Tomas et al., 2006; Tzeng et al., 1999), our results can help to advance the interpretation of visual growth marks and improve age estimation.

CRediT authorship contribution statement

Deirdre Brophy: Conceptualization, Methodology, Formal analysis, Writing- Original draft preparation, Visualization, Supervision, Project administration, Funding acquisition. **Sílvia Pérez-Mayol:** Conceptualization, Methodology, Investigation, Formal analysis, Writing- Original draft preparation, Funding acquisition. **Roxanne Duncan:** Investigation, Formal analysis, Writing - review & editing. **Karin Hüssy:** Conceptualization, Methodology, Writing - review & editing, Funding acquisition. **Audrey J. Geffen:** Conceptualization, Methodology, Formal analysis, Writing - review & editing, Funding acquisition. **Hans D. Gerritsen:** Conceptualization, Methodology, Investigation, Writing - review & editing, Funding acquisition. **Maria Ching Villanueva:** Conceptualization, Investigation, Writing - review & editing, Funding acquisition. **Beatriz Morales-Nin:** Conceptualization, Methodology, Writing- Original draft preparation, Funding acquisition.

Declaration of competing interest

The authors declare that they have no known competing financial interests or personal relationships that could have appeared to influence the work reported in this paper.

Acknowledgements

This work was performed as part of a contract to the Executive Agency to Small and Medium-sized Enterprises (EASME) of the European Commission (EASME/EMFF/2016/1.3.2.7/SI2.762036). SPM's salary was co-funded by the DGPUR of the Balearic Government and CSIC. The analytical services at the University of the Balearic Islands and A Coruña University are thanked for the support provided. The authors are grateful to all personnel involved in the collection of samples, particularly Marcin Blaszkowski.

Appendix A. Supplementary data

Supplementary data to this article can be found online at https://doi.org/10.1016/j.ecss.2021.107557.

References

Allen, P.J., Hobbs, J.A., Cech, J.J., Van Eenennaam, J.P., Doroshov, S.I., 2009. Using trace elements in pectoral fin rays to assess life history movements in sturgeon: estimating age at initial seawater entry in Klamath River green sturgeon. Trans. Am. Fish. Soc. 138, 240–250. https://doi.org/10.1577/T08-061.1.

Arai, T., Levin, A.V., Boltunov, A.N., Miyazaki, N., 2002. Migratory history of the Russian sturgeon *Acipenser guldenstadti* in the Caspian Sea, as revealed by pectoral fin spine Sr : Ca ratios. Marine Biology 141, 315–319. https://doi.org/10.1007/s00227-002-0820-y.

Barcala, E., Bellido, J.M., Bellodi, A., Carbonara, P., Carlucci, R., Casciaro, L., Esteban, A., Jadaud, A., Massaro, A., Peristaki, P., Melendez, M.J., Gil, J.L.P., Salmeron, F., Pennino, M.G., 2019. Spatio-temporal variability in the distribution pattern of anglerfish species in the Mediterranean Sea. Sci. Mar. 83, 129–139. https://doi.org/10.3989/scimar.04966.11A.

Bates, D., Machler, M., Bolker, B.M., Walker, S.C., 2015. Fitting linear mixed-effects models using lme4. J. Stat. Software 67, 1–48. https://doi.org/10.18637/jss.v067.i01.

Bath, G.E., Thorrold, S.R., Jones, C.M., Campana, S.E., McLaren, J.W., Lam, J.W.H., 2000. Strontium and barium uptake in aragonitic otoliths of marine fish. Geochem. Cosmochim. Acta 64, 1705–1714. https://doi.org/10.1016/S0016-7037(99)00419-6.

Batts, L., Minto, C., Gerritsen, H., Brophy, D., 2019. Estimating growth parameters and growth variability from length frequency data using hierarchical mixture models. ICES J. Mar. Sci. 76, 2150–2163. https://doi.org/10.1093/icesjms/fsz103.

Catalán, I.A., Alós, J., Díaz-Gil, C., Pérez-Mayol, S., Basterretxea, G., Morales-Nin, B., Palmer, M., 2018. Potential fishing-related effects on fish life history revealed by otolith microchemistry. Fish. Res. 199, 186–195. https://doi.org/10.1016/j.fishres.2017.11.008.

Clarke, A.D., Telmer, K.H., Shrimpton, J.M., 2007. Elemental analysis of otoliths, fin rays and scales: a comparison of bony structures to provide population and life-history information for the Arctic grayling (*Thymallus arcticus*). Ecol. Freshw. Fish 16, 354–361. https://doi.org/10.1111/j.1600-0633.2007.00232.x.

Clarke, L.M., Friedland, K.D., 2004. Influence of growth and temperature on strontium deposition in the otoliths of Atlantic salmon. J. Fish Biol. 65, 744–759. https://doi.org/10.1111/j.0022-1112.2004.00480.x.

Crozier, W.W., 1989. Age and growth of angler-fish (*Lophius piscatorius* L.) in the north Irish Sea. Fish. Res. 7, 267–278. https://doi.org/10.1016/0165-7836(89)90060-X.

Davies, C.A., Brophy, D., Jeffries, T., Gosling, E., 2011. Trace elements in the otoliths and dorsal spines of albacore tuna (*Thunnus alalunga*, Bonnaterre, 1788): an assessment of the effectiveness of cleaning procedures at removing postmortem contamination. J. Exp. Mar. Biol. Ecol. 396, 162–170. https://doi.org/10.1016/j.jembe.2010.10.016.

Doubleday, Z.A., Harris, H.H., Izzo, C., Gillanders, B.M., 2014. Strontium randomly substituting for calcium in fish otolith aragonite. Anal. Chem. 86, 865–869. https://doi.org/10.1021/ac4034278.

Duarte, R, Landa, J, Quincoces, I, Dupouy, H, Bilbao, E, Dimeet, J, Marçal, A, McCormick, H, Ní Chonchúir, G, 2002. Anglerfish Ageing Guide. Report of the 4th International Ageing Workshop on European Anglerfish. IPIMAR, Lisbon, Portugal, pp. 73–112.

Elsdon, T.S., Gillanders, B.M., 2002. Interactive effects of temperature and salinity on otolith chemistry: challenges for determining environmental histories of fish. Can. J. Fish. Aquat. Sci. 59, 1796–1808. https://doi.org/10.1139/f02-154.

Elsdon, T.S., Gillanders, B.M., 2005. Strontium incorporation into calcified structures: separating the effects of ambient water concentration and exposure time. Mar. Ecol. Prog. Ser. 285, 233–243. https://doi.org/10.3354/meps285233.

FAO, 2019. FAO yearbook. Fishery and Aquaculture Statistics 2017/FAO annuaire. Statistiques des pêches et de l'aquaculture 2017/FAO anuario. Estadísticas de pesca y acuicultura 2017, Rome/Roma.

Fariña, A.C., Duarte, R.A.M., Landa, J., Quincoces, I., Sánchez, J.A., 2004. Multiple Stock Identification Approaches of Anglerfish (*Lophius Piscatorius* and *L . Budegassa*) in Western and Southern European Waters. ICES Document CM 2004/EE, p. 25.

Feldlite, M., Juanico, M., Karplus, I., Milstein, A., 2008. Towards a safe standard for heavy metals in reclaimed water used for fish aquaculture. Aquaculture 284, 115–126. https://doi.org/10.1016/j.aquaculture.2008.07.036.

Francis, R, 1990. Back-calculation of fish length - a critical review. J. Fish Biol. 36, 883–902. https://doi.org/10.1111/j.1095-8649.1990.tb05636.x.

Gillanders, B.M., 2001. Trace metals in four structures of fish and their use for estimates of stock structure. Fish. Bull. 99, 410–419.

Gillanders, B.M., 2005. Using elemental chemistry of fish otoliths to determine connectivity between estuarine and coastal habitats. Estuar. Coast. Shelf Sci. 64, 47–57. https://doi.org/10.1016/j.ecss.2005.02.005.

Good, S.A., Martin, M.J., Rayner, N.A., 2013. EN4: quality controlled ocean temperature and salinity profiles and monthly objective analyses with uncertainty estimates. J. Geophys. Res.: Oceans 118, 6704–6716. https://doi.org/10.1002/2013jc009067.

Granzotto, A., Franceschini, G., Malavasi, S., Molin, G., Pranovi, F., Torricelli, P., 2003. Marginal increment analysis and Sr/Ca ratio in otoliths of the grass goby, *Zosterisessor ophiocephalus*. Ital. J. Zool. 70, 5–11. https://doi.org/10.1080/11250000309356489.

Günther, D., Jackson, S.E., Longerich, H.P., 1999. Laser ablation and arc/spark solid sample introduction into inductively coupled plasma mass spectrometers. Spectrochim. Acta B Atom. Spectrosc. 54, 381–409. https://doi.org/10.1016/S0584-8547(99)00011-7.

Heimbrand, Y., Limburg, K.E., Hussy, K., Casini, M., Sjoberg, R., Bratt, A.M.P., Levinsky, S.E., Karpushevskaia, A., Radtke, K., Ohlund, J., 2020. Seeking the true time: exploring otolith chemistry as an age-determination tool. J. Fish Biol. 97, 552–565. https://doi.org/10.1111/jfb.14422.

Hislop, J.R.G., Holst, J.C., Skagen, D., 2000. Near-surface captures of post-juvenile anglerfish in the North-east Atlantic - an unsolved mystery. J. Fish Biol. 57, 1083–1087. https://doi.org/10.1006/jfbi.2000.1364.

Hüssy, K., Gröger, J., Heidemann, F., Hinrichsen, H.H., Marohn, L., 2015. Slave to the rhythm: seasonal signals in otolith microchemistry reveal age of eastern Baltic cod (*Gadus morhua*). ICES J. Mar. Sci. 73, 1019–1032. https://doi.org/10.1093/icesjms/fsv247.

Hüssy, K., Limburg, K.E., de Pontual, H., Thomas, O.R.B., Cook, P.K., Heimbrand, Y., Blass, M., Sturrock, A.M., 2020. Trace element patterns in otoliths: the role of biomineralization. Rev. Fish. Sci. Aquacult. https://doi.org/10.1080/23308249.2020.1760204.

ICES, 2011. Report of the Anglerfish (*Lophius Piscatorius*) Illicia and Otoliths Exchange 2011. ICES Planning Group on Commercial Catch, Discards and Biological Sampling.

ICES, 2018. Report of the Benchmark Workshop on Anglerfish Stocks in the ICES Area (WKANGLER), 12–16 February 2018, Copenhagen, Denmark. ICES CM 2018/ACOM: 31. 177pp.

Jaric, I., Lenhardt, M., Pallon, J., Elfman, M., Kalauzi, A., Suciu, R., Cvijanovic, G., Ebenhard, T., 2011. Insight into Danube sturgeon life history: trace element assessment in pectoral fin rays. Environ. Biol. Fish. 90, 171–181. https://doi.org/10.1007/s10641-010-9728-4.

Kalish, J.M., 1991. Determinants of otolith chemistry - seasonal-variation in the composition of blood-plasma, endolymph and otoliths of bearded rock cod *Pseudophycis barbatus*. Marine Ecology-Progress Series 74, 137–159. https://doi.org/10.3354/meps074137.

Kastelle, C.R., Helser, T.E., McKay, J.L., Johnston, C.G., Anderl, D.M., Matta, M.E., Nichol, D.G., 2017. Age validation of Pacific cod (*Gadus macrocephalus*) using high-resolution stable oxygen isotope ($\delta^{18}O$) chronologies in otoliths. Fish. Res. 185, 43–53. https://doi.org/10.1016/j.fishres.2016.09.024.

Kennedy, B.P., Blum, J.D., Folt, C.L., Nislow, K.H., 2000. Using natural strontium isotopic signatures as fish markers: methodology and application. Can. J. Fish. Aquat. Sci. 57, 2280–2292. https://doi.org/10.1139/f00-206.

Köck, G., Noggler, M., Hofer, R., 1996. Pb in otoliths and opercula of Arctic char (*Salvelinus alpinus*) from oligotrophic lakes. Water Res. 30, 1919–1923. https://doi.org/10.1016/0043-1354(96)00074-7.

Kraus, R.T., Secor, D.H., 2004. Incorporation of strontium into otoliths of an estuarine fish. J. Exp. Mar. Biol. Ecol. 302, 85–106. https://doi.org/10.1016/j.jembe.2003.10.004.

Kuznetsova, A., Brockhoff, P.B., Christensen, R.H.B., 2017. Lmertest package: tests in linear mixed effects models. J. Stat. Software 82, 1–26. https://doi.org/10.18637/jss.v082.i13.

Landa, J., Barrado, J., Velasco, F., 2013. Age and growth of anglerfish (*Lophius piscatorius*) on the Porcupine Bank (west of Ireland) based on illicia age estimation. Fish. Res. 137, 30–40. https://doi.org/10.1016/j.fishres.2012.07.026.

Landa, J., Duarte, R., Quincoces, I., 2008. Growth of white anglerfish (*Lophius piscatorius*) tagged in the Northeast Atlantic, and a review of age studies on anglerfish. ICES J. Mar. Sci. 65, 72–80. https://doi.org/10.1093/icesjms/fsm170.

Laurenson, C.H., Johnson, A., Priede, I.G., 2005. Movements and growth of monkfish *Lophius piscatorius* tagged at the Shetland Islands, northeastern Atlantic. Fish. Res. 71, 185–195. https://doi.org/10.1016/j.fishres.2004.08.020.

Lenth, R., 2020. emmeans: estimated marginal means, aka least-squares means. R package version 1.5.2-1. https://CRAN.R-project.org/package=emmeans.

Limburg, K.E., Elfman, M., 2017. Insights from two-dimensional mapping of otolith chemistry. J. Fish Biol. 90, 480–491. https://doi.org/10.1111/jfb.13048.

Luque, P.L., Zhang, S., Rooker, J.R., Bidegain, G., Rodriguez-Marin, E., 2017. Dorsal fin spines as a non-invasive alternative calcified structure for microelemental studies in Atlantic bluefin tuna. J. Exp. Mar. Biol. Ecol. 486, 127–133. https://doi.org/10.1016/j.jembe.2016.09.016.

Macdonald, J., Drysdale, R., Witt, R., Csagoly, Z., Marteinsdottir, G., 2020. Isolating the influence of ontogeny helps predict island-wide variability in fish otolith chemistry. Rev. Fish Biol. Fish. 30 https://doi.org/10.1007/s11160-019-09591-x.

Maunder, M.N., Piner, K.R., 2014. Contemporary fisheries stock assessment: many issues still remain. ICES J. Mar. Sci. 72, 7–18. https://doi.org/10.1093/icesjms/fsu015.

McFadden, A., Wade, B., Izzo, C., Gillanders, B.M., Lenehan, C.E., Pring, A., 2016. Quantitative electron microprobe mapping of otoliths suggests elemental incorporation is affected by organic matrices: implications for the interpretation of otolith chemistry. Mar. Freshw. Res. 67, 889–898. https://doi.org/10.1071/MF15074.

Miller, J.A., Hurst, T.P., 2020. Growth rate, ration, and temperature effects on otolith elemental incorporation. Frontiers in Marine Science 7, 320. https://doi.org/10.3389/fmars.2020.00320.

Morales-Nin, B., Geffen, A.J., Pérez-Mayol, S., Palmer, M., González-Quirós, R., Grau, A., 2012. Seasonal and ontogenic migrations of meagre (*Argyrosomus regius*) determined by otolith geochemical signatures. Fish. Res. 127–128, 154–165. https://doi.org/10.1016/j.fishres.2012.02.012.

Morales-Nin, B., Pérez-Mayol, S., Palmer, M., Geffen, A.J., 2014. Coping with connectivity between populations of *Merluccius merluccius*: an elusive topic. J. Mar. Syst. 138, 211–219. https://doi.org/10.1016/j.jmarsys.2014.04.009.

Morrongiello, J.R., Thresher, R.E., 2014. A statistical framework to explore ontogenetic growth variation among individuals and populations: a marine fish example. Ecol. Monogr. 85, 93–115. https://doi.org/10.1890/13-2355.1.

Mugiya, Y., Satoh, C., 1997. Strontium accumulation in slow-growing otoliths in the goldfish *Carassius auratus*. Fish. Sci. 63, 361–364. https://doi.org/10.2331/FISHSCI.63.361.

Nakagawa, S, Schielzeth, H, 2013. A general and simple method for obtaining R^2 from generalized linear mixed-effects models. Methods Ecol. Evol. 4, 133–142. https://doi.org/10.1111/j.2041-210x.2012.00261.x.

Phelps, Q.E., Whitledge, G.W., Tripp, S.J., Smith, K.T., Garvey, J.E., Herzog, D.P., Ostendorf, D.E., Ridings, J.W., Crites, J.W., Hrabik, R.A., Doyle, W.J., Hill, T.D., 2012. Identifying river of origin for age-0 Scaphirhynchus sturgeons in the Missouri and Mississippi rivers using fin ray microchemistry. Can. J. Fish. Aquat. Sci. 69, 930–941. https://doi.org/10.1139/f2012-038.

Pollard, M.J., Kingsford, M.J., Battaglene, S.C., 1999. Chemical marking of juvenile snapper, *Pagrus auratus* (Sparidae), by incorporation of strontium into dorsal spines. Fish. Bull. 97, 118–131.

Quéro, J.C., Vayne, J.J., 2005. Les poissons de mer des pêches françaises : inventaire, identification et répartition de 209 espèces de poissons de mer des pêches françaises. Lonay (Suisse).

R Core Team, 2020. R: A Language and Environment for Statistical Computing. R Foundation for Statistical Computing, Vienna, Austria. URL. https://www.R-project.org/.

Reis-Santos, P., Tanner, S.E., Elsdon, T.S., Cabral, H.N., Gillanders, B.M., 2013. Effects of temperature, salinity and water composition on otolith elemental incorporation of *Dicentrarchus labrax*. J. Exp. Mar. Biol. Ecol. 446, 245–252. https://doi.org/10.1016/j.jembe.2013.05.027.

Rude, N.P., Smith, K.T., Whitledge, G.W., 2014. Identification of stocked muskellunge and potential for distinguishing hatchery-origin and wild fish using pelvic fin ray microchemistry. Fish. Manag. Ecol. 21, 312–321. https://doi.org/10.1111/fme.12081.

Sadovy, Y., Severin, K.P., 1994. Elemental patterns in red hind (*Epinephelus guttatus*) otoliths from Bermuda and Puerto Rico reflect growth-rate, not temperature. Can. J. Fish. Aquat. Sci. 51, 133–141. https://doi.org/10.1139/f94-015.

Sanborn, M., Telmer, K., 2003. The spatial resolution of LA-ICP-MS line scans across heterogeneous materials such as fish otoliths and zoned minerals. J. Anal. At. Spectrom. 18, 1231–1237. https://doi.org/10.1039/B302513F.

Scharer, R.M., Patterson, W.F., Carlson, J.K., Poulakis, G.R., 2012. Age and growth of endangered smalltooth sawfish (pristis pectinata) verified with la-icp-ms analysis of vertebrae. PloS One 7 (10), e47850. https://doi.org/10.1371/journal.pone.0047850, 7.

Seyama, H, Edmonds, J.S., Moran, M.J., Shibata, Y, Soma, M, Morita, M, 1991. Periodicity in fish otolith Sr, Na, and K corresponds with visual banding. Experientia 47, 1193–1196. https://doi.org/10.1007/BF01918383.

Siskey, M.R., Lyubchich, V., Liang, D., Piccoli, P.M., Secor, D.H., 2016. Periodicity of strontium: calcium across annuli further validates otolith-ageing for Atlantic bluefin tuna (*Thunnus thynnus*). Fish. Res. 177, 13–17. https://doi.org/10.1016/j.fishres.2016.01.004.

Smith, K.T., Whitledge, G.W., 2010. Fin ray chemistry as a potential natural tag for smallmouth bass in northern Illinois Rivers. J. Freshw. Ecol. 25, 627–635. https://doi.org/10.1080/02705060.2010.9664412.

Smith, K.T., Whitledge, G.W., 2011. Evaluation of a stable-isotope labelling technique for mass marking fin rays of age-0 lake sturgeon. Fish. Manag. Ecol. 18, 168–175. https://doi.org/10.1111/j.1365-2400.2010.00771.x.

Somers, I.F., 1988. On a seasonally oscillating growth function. Fishbyte 6 (1), 8–11.

Sturgeon, R.E., Willie, S.N., Yang, L., Greenberg, R., Spatz, R.O., Chen, Z., Scriver, C., Clancy, V., Lam, J.W., Thorrold, S., 2005. Certification of a fish otolith reference material in support of quality assurance for trace element analysis. J. Anal. At. Spectrom. 20, 1067–1071. https://doi.org/10.1039/B503655K.

Sturrock, A., Trueman, C., Milton, J., Waring, C., Cooper, M., Hunter, E., 2014. Physiological influences can outweigh environmental signals in otolith microchemistry research. Mar. Ecol. Prog. Ser. 500, 245–264. https://doi.org/10.3354/meps10699.

Sturrock, A.M., Hunter, E., Milton, J.A., Eimf, Johnson, R.C., Waring, C.P., Trueman, C. N., 2015. Quantifying physiological influences on otolith microchemistry. Methods Ecol. and Evol. 6, 806–816. https://doi.org/10.1111/2041-210X.12381.

Thangstad, T., Bjelland, O., Nedreaas, K., Jónsson, E., Laurenson, C., Ofstad, L., 2006. Anglerfish (*Lophius* Spp) in Nordic Waters. TemaNord 2006: 570. Nordic Council of Ministers, Copenhagen.

Tillett, B.J., Meekan, M.G., Parry, D., Munksgaard, N., Field, I.C., Thorburn, D., Bradshaw, C.J.A., 2011. Decoding fingerprints: elemental composition of vertebrae correlates to age-related habitat use in two morphologically similar sharks. Mar. Ecol. Prog. Ser. 434, 133–143. https://doi.org/10.3354/meps09222.

Tomas, J., Geffen, A.J., Millner, R.S., Pineiro, C.G., Tserpes, G., 2006. Elemental composition of otolith growth marks in three geographically separated populations of European hake (*Merluccius merluccius*). Mar. Biol. 148, 1399–1413. https://doi.org/10.1007/s00227-005-0171-6.

Townsend, D.W., Radtke, R.L., Corwin, S., Libby, D.A., 1992. Strontium:calcium ratios in juvenile Atlantic herring *Clupea harengus* L. otoliths as a function of water temperature. J. Exp. Mar. Biol. Ecol. 160, 131–140. https://doi.org/10.1016/0022-0981(92)90115-Q.

Tzeng, W.N., Severin, K.P., Wickstrom, H., Wang, C.H., 1999. Strontium bands in relation to age marks in otoliths of European eel *Anguilla anguilla*. Zool. Stud. 38, 452–457.

Ugarte, A., Abrego, Z., Unceta, N., Goicolea, M.A., Barrio, R.J., 2012. Evaluation of the bioaccumulation of trace elements in tuna species by correlation analysis between their concentrations in muscle and first dorsal spine using microwave-assisted digestion and ICP-MS. Int. J. Environ. Anal. Chem. 92, 1761–1775. https://doi.org/10.1080/03067319.2011.603078.

Ugarte, A., Unceta, N., Pecheyran, C., Goicolea, M.A., Barrio, R.J., 2011. Development of matrix-matching hydroxyapatite calibration standards for quantitative multi-element LA-ICP-MS analysis: application to the dorsal spine of fish. Journal of Analytical Atomic Spectrometry 26, 1421–1427. https://doi.org/10.1039/C1JA10037H.

Vas, P., 1991. Trace-metal levels in sharks from British and Atlantic waters. Mar. Pollut. Bull. 22, 67–72. https://doi.org/10.1016/0025-326X(91)90138-I.

Veinott, G., Northcote, T., Rosenau, M., Evans, R.D., 1999. Concentrations of strontium in the pectoral fin rays of the white sturgeon (*Acipenser transmontanus*) by laser ablation sampling - inductively coupled plasma - mass spectrometry as an indicator of marine migrations. Can. J. Fish. Aquat. Sci. 56, 1981–1990. https://doi.org/10.1139/cjfas-56-11-1981.

Velasco, F., Landa, J., Barrado, J., Blanco, M., 2008. Distribution, abundance, and growth of anglerfish (*Lophius piscatorius*) on the Porcupine Bank (west of Ireland). ICES J. Mar. Sci. 65, 1316–1325.

Vitale, F., Worsøe Clausen, L., Ní Chonchúir, G.E., 2019. Handbook of fish age estimation protocols and validation methods. ICES Cooperative Research Report No. 346. http://doi.org/10.17895/ices.pub.5221, 180.

Walther, B.D., 2019. The art of otolith chemistry: interpreting patterns by integrating perspectives. Mar. Freshw. Res. 70, 1643–1658. https://doi.org/10.1071/MF18270.

Walther, B.D., Kingsford, M.J., O'Callaghan, M.D., McCulloch, M.T., 2010. Interactive effects of ontogeny, food ration and temperature on elemental incorporation in otoliths of a coral reef fish. Environ. Biol. Fish. 89, 441–451. https://doi.org/10.1007/s10641-010-9661-6.

Walther, B.D., Thorrold, S.R., 2006. Water, not food, contributes the majority of strontium and barium deposited in the otoliths of a marine fish. Mar. Ecol. Prog. Ser. 311, 125–130. https://doi.org/10.3354/meps311125.

Whitehead, P.J.P., Bauchot, M.L., Hureau, J.C., Nielsen, J., Tortonese, E., 1986. Fishes of the North-eastern Atlantic and the Mediterranean Poissons de l'Atlantique du Nord-Est et de la Méditerranée. UNESCO.

Wickham, H., 2016. ggplot2: Elegant Graphics for Data Analysis. Springer-Verlag, New York.

Wolff, B.A., Johnson, B.M., Landress, C.M., 2013. Classification of hatchery and wild fish using natural geochemical signatures in otoliths, fin rays, and scales of an endangered catostomid. Can. J. Fish. Aquat. Sci. 70, 1775–1784. https://doi.org/10.1139/cjfas-2013-0116.

Woodroffe, D.A., Wright, P.J., Gordon, J.D.M., 2003. Verification of annual increment formation in the white anglerfish, *Lophius piscatorius* using the illicia and sagitta otoliths. Fish. Res. 60, 345–356. https://doi.org/10.1016/S0165-7836(02)00174-1.

Wright, P.J., Woodroffe, D.A., Gibb, F.M., Gordon, J.D.M., 2002. Verification of first annulus formation in the illicia and otoliths of white anglerfish, *Lophius piscatorius* using otolith microstructure. ICES (Int. Counc. Explor. Sea) J. Mar. Sci. 59, 587–593. https://doi.org/10.1006/jmsc.2002.1179.

Yoshinaga, J., Nakama, A., Morita, M., Edmonds, J.S., 2000. Fish otolith reference material for quality assurance of chemical analyses. Mar. Chem. 69, 91–97. https://doi.org/10.1016/S0304-4203(99)00098-5.

Zeileis, A., Hothorn, T., 2002. Diagnostic checking in regression relationships. R. News 2, 7–10. https://cran.r-project.org/web/packages/lmtest/vignettes/lmtest-intro.pdf.